АСТРОФИЗИКА

ТОМ 62 МАЙ, 2019 ВЫПУСК 2

ACTIVITY TYPES OF GALAXIES SELECTED FROM HRC/BHRC SAMPLE

G.M.PARONYAN[1], A.M.MICKAELIAN[1], G.S.HARUTYUNYAN[2], H.V.ABRAHAMYAN[1], G.A.MIKAYELYAN[1]

Received 25 April 2018
Accepted 13 March 2019

In this study we carry out detailed spectral classification of 173 AGN candidates from the Joint HRC/BHRC sample, which is a combination of HRC (Hamburg-ROSAT Catalogue) and BHRC (Byurakan-Hamburg-ROSAT Catalogue). These objects were revealed as optical counterparts for ROSAT X-ray sources, however spectra for 173 of them are given in SDSS without definite spectral classification. We studied these 173 objects using the SDSS spectra and revealed the detailed activity types for them. Three diagnostic diagrams and direct examination of the spectra were used to have more confident classification. We also made identification of these sources in other wavelength ranges and calculated some of their parameters.

Keywords: *AGN: X-ray: spectral classification: HRC/BHRC: X-ray AGN*

1. *Introduction*. The ROSAT satellite was equipped with a mirror of 84 cm diameter and an X-ray detector having sensitivity between 0.1-2.4 keV. With this satellite a whole sky survey was accomplished in X-ray. ROSAT data are mainly listed in two catalogs: ROSAT Bright Source Catalogue (BSC) [1] and ROSAT Faint Source Catalogue (FSC) [2]. They are clearly distinguished from each other by X-ray flux expressed in count-rate (CR; the number of particles registered by the receiver per unit time, namely per 1 sec). ROSAT-BSC contains 18811 sources with $CR > 0.05$ ct/s, while ROSAT-FSC, 105924 sources with $CR < 0.05$ ct/s with a sensitivity limit $CR < 0.0005$ ct/s. Thus, ROSAT catalogues contain 124735 X-ray sources. There are thousands of interesting objects among them, and even though a number of recent X-ray missions have been conducted (Chandra, XMM and others), ROSAT so far remains the only all-sky enough deep survey, particularly containing some 60000-70000 X-ray AGN. However, only 10000 ROSAT sources have been optically identified.

To ensure the homogeneity and completeness of the sample, only data from ROSAT catalogues have been taken for X-ray sources.

Among the identification works, the ROSAT Bright Sources (RBS, [3]) is well-known. 2012 BSC sources with $CR \geq 0.20$ and $|b| > 30^\circ$ have been optically identified. However, most of the identified sources come from the Hamburg Quasar

Survey (HQS, |4|), which was used as a basis for optical identifications. This survey was accomplished by the Hamburg Observatory Schmidt telescope with a diameter of 80 cm and covers the entire northern sky at high Galactic latitudes. Spectra were obtained using a wide-angle prism (1°.7). 1931 Kodak IIIa-J emulsion plates were used for observation with spectral sensitivity between 3400–5400 Å. HQS low-dispersion spectra allow a preliminary classification of objects into a number of types, giving possibility to make up subsamples of objects for further studies. Two main projects have been carried out: Hamburg-ROSAT Catalogue (HRC, |5|) and Byurakan-Hamburg-ROSAT Catalogue (BHRC, |6|). HRC is based on ROSAT-BSC and contains 5341 sources at $|b| > 20°$ and $\delta > 0°$, while BHRC is based on ROSAT-FSC and contains 2791 fainter sources (down to CR = 0.04 to have confident X-ray sources) in the same area (3297 objects found, including many binaries).

In both catalogues, the selection of optical sources was made due to the following advantages of HQS:

1. The survey covers the entire extragalactic northern sky with $\delta > 0°$ and $|b| > 20°$;
2. Spectra were received with the help of an objective prism with a dispersion 1390 Å /mm allowing follow spectral energy distribution (SED) and notice some broad emission and absorption lines;
3. All plates of the survey are digitized with high quality and are accessible for studies;
4. HQS allows a quick identification of objects and finding their data in other catalogues.

Among the 5341 HRC optical identifications, 1607 are given as AGN or their candidates and among the 2696 BHRC objects, there are 1614 considered to be AGN or their candidates.

We combined these two Catalogues and created a new homogeneous and complete catalogue of X-ray selected AGN, which covers all the northern sky limited by high galactic latitudes ($\delta > 0°$, $|b| \geq 20°$), and with CR > 0.04. After some checks from various available catalogs, we have excluded a number of objects and included some missed AGN and finally it contained 4253 AGN or their candidates.

We cross-matched the Catalogue of QSOs and Active Nuclei, Version 13 (hereafter VCV-13) [7]. VCV-13 includes only those objects, which have optical spectra and their spectroscopic studies confirmed their AGN nature. It contains 168940 AGN. To complement VCV-13, we also used BZCAT |8| due to its better completeness for blazars (high probability X-ray sources). Though at present many new QSOs and other AGN have been discovered from SDSS recent releases |9| and some other works, however most of them are faint objects and do not strongly contribute to identifications of more ROSAT sources.

Out of the 4253 HRC-BHRC objects, 3369 sources were confirmed as AGN by means of optical spectral classifications; the main criteria in VCV-13 and BZCAT, and the rest 884 are left as AGN candidates.

Out of these 884, for 173 AGN candidates in our sample there are spectra from SDSS; we are carrying out a detailed spectral classification thus introducing new AGN or rejecting some objects.

We have carried out cross-correlations of our sample with the recent all-sky and large-area catalogues.

To determine the correct search radius for all cross-correlations and avoid misidentifications, a preliminary identification was made with a large radius, and then the distribution of distances of identifications was constructed for all sources. This allowed determine the correct search radius. Fig.1 gives an example of such computation for SDSS catalogue. We conclude that objects with distances from the input positions up to 1.5 arcsec should be considered as genuine associations, though the real search radii were taken larger not to miss some genuine associations having larger positional errors.

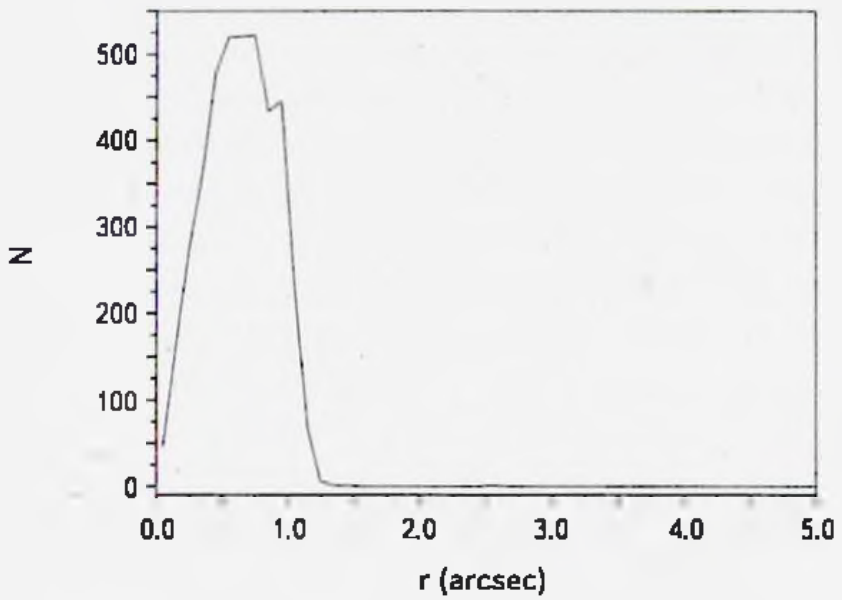

Fig.1. Computation of the correct radius of identifications for SDSS catalogue.

If during the identification, we had several objects corresponding to the given source, we selected the source, which was 3 times closer than the second one as a confident identification. And if the ratio of distances was smaller and it was not possible to identify a reliable source, a flag with <:> sign is given, which means a doubtful identification.

2. *Observing material.* As observing material we had 173 spectra of HRC-BHRC objects from SDSS DR7 [10], DR8 and DR9. Spectroscopic redshifts,

intensities (assigned as "heights") and equivalent widths of spectral lines for 173 of them from SDSS DR7-DR9 are available. The wavelength range of all spectra is 3800-9200 Å, the resolution is R = 1800 - 2200, signal to noise ratio (S/N) is better than 4 per pixel at g = 20.2, redshift accuracy is 30 km/s rms, radial velocity accuracy is typically 5.5 km/s rms. As a rule, most of these spectra have good quality with S/N ratio better than 5 and only a few spectra are worse.

As SDSS observations have used the same size of the fiber, most of the resolved galaxies appeared to have absorption components and only very few show pure nuclear spectra. Most typical absorption lines are Mg II 5175 Å, Na I 5890 Å and Balmer lines among which most important are Hβ absorption components superposed on the emission components coming from nuclei. Due to redshifts in the SDSS spectral range usually following emission lines appear: [OII] 3727 Å, Hζ/HeI 3889 Å, [NeIII] 3968 Å, Hε, [SII] 4069/76 Å, Hδ, Hγ, [OIII] 4363 Å, Hβ, [OIII] 4959 Å, [OIII] 5007 Å, NI 5198/5200 Å, HeI 5876 Å, [OI] 6300 Å, [OI] 6364 Å, [NII] 6548 Å, Hα, [NII] 6583 Å, [SII] 6716 Å, [SII] 6731 Å.

Very often SDSS measurements from their spectra are based on very low-quality lines at the level of noise. These automatic measurements give some artificial numbers that indicate non-real data. So, one needs to carefully check the spectra along all wavelengths and decide which measurements should be used for further studies. Especially important are those, which are being used in the diagnostic diagrams (Hβ, [OIII] 5007 Å, [OI] 6300 Å, Hα, [NII] 6583 Å, and [SII] 6716+6731 Å) [11].

3. *Classification principles*. We have used several methods for classification of our spectra: by eye examination (taking into account all features and effects), by diagnostic diagrams using [OIII]/Hβ and [OI]/Hα ratios, [OIII]/Hβ and [NII]/Hα ratios, [OIII]/Hβ and [SII]/Hα ratios.

Classification by eye has been done to compare with the classification by diagnostic diagrams and because not all objects appeared on them. Besides, the broad emission line component is not taken into account on the diagnostic diagrams, and this may be crucial for the classification of Seyfert 1.2-1.9 subclasses. Roughly, we distinguish Seyferts from LINERs by the criteria: $[OIII]/H\beta > 4$, and AGN from HII by $[NII]/H\alpha > 2/3$, $[OI]/H\alpha > 0.1$ criteria.

Following activity classes appear among our objects:

S1.0. Broad-line Seyfert 1. Have broad permitted Balmer HI lines and narrow forbidden lines. Physically are the same objects as QSOs but having smaller luminosities (M_{abs} >-23) [12] and Hβ/[OIII]5007 > 5.0 [13].

NLS1.0. Narrow-line Seyfert 1. Defined by [14] as soft X-ray sources, having narrow permitted lines only slightly broader than the forbidden ones; many FeI, FeII, FeIII, and often strong [FeVII] and [FeX] emission lines are present.

Introduced by Osterbrock&Pogge in 1985 [14].

S1.2. Spectra of AGN, which share parameters that are intermediate between those of classical Sy1 and Sy2 galaxies, i.e. both broad and narrow components are present for permitted lines (in our case Hα and Hβ lines display such profiles) [12], however, broad lines are stronger, and $2.0 < H\beta/[OIII]5007 < 5.0$ [13].

NLS1.2. Narrow-line Seyfert 1.2. Have is soft X-ray sources, having narrow permitted lines only slightly broader than the forbidden ones; many FeI, FeII, FeIII, and often strong [FeVII] and [FeX] emission lines present.

S1.5. Spectra of AGN which share parameters that are intermediate between those of classical Sy1 and Sy2 galaxies, have easily discernible narrow HI profile superposed on broad wings [12], but $0.333 < H\beta/[OIII]5007 < 2.0$ [13]. Broad and narrow components are approximately equal in intensity.

NLS1.5. Narrow-line Seyfert 1.5. These are soft X-ray sources, having narrow permitted lines only slightly broader than the forbidden ones; many FeI, FeII, FeIII, and often strong [FeVII] and [FeX] emission lines present.

S1.8. AGN which share parameters that are intermediate between those of classical Sy1 and Sy2 galaxies; have relatively weak broad Hα and Hβ components superposed on strong narrow lines, and $H\beta/[OIII]5007 < 0.333$ [13].

NLS1.8. Narrow-line Seyfert 1.8. This is soft X-ray sources, having narrow permitted lines only slightly broader than the forbidden ones; many FeI, FeII, FeIII, and often strong [FeVII] and [FeX] emission lines present.

S1.9. Spectra of AGN which share parameters that are intermediate between those of classical Sy1 and Sy2 galaxies, have relatively weak broad Hβ component superposed on a strong narrow line. The broad component of Hβ is not seen [12], and $H\beta/[OIII]5007 < 0.333$ [13].

NLS1.9. Narrow-line Seyfert 1.9. This is soft X-ray sources, having narrow permitted lines only slightly broader than the forbidden ones; many FeI, FeII, FeIII, and often strong [FeVII] and [FeX] emission lines present.

S2.0. Spectra of AGN that show relatively narrow (compared to Sy1) emission in both permitted Ballmer and forbidden lines, with almost the same FWHM, typically in the range of 300-1000 km/s. No broad component is visible. A secondary classification criterion is $[OIII]5007/H\beta \geq 3$, to distinguish against Sy1n [11].

LINER. Have Sy2-like spectra with relatively strong low-ionization lines ([OI], [OII]) [15]. According to Ho et al. [16], there are 2 classes of LINERS: type 1 show broad Balmer emission in analogy with Sy1s, and type 2, without broad Ha in analogy with Sy2s.

HII. Extragalactic HII regions. Have spectra similar to SB that is a strong narrow (FWHM $\leq$ 300 km/s) emission line spectrum but with a ratio $[OIII]/H\beta \geq 3$ and $[NII]6584/H\alpha < 0.5$, coupled with a blue continuum [12,18].

Composite (mixture of HII/LINER, HII/Seyfert or LINER/Seyfert features).

Composite spectrum objects with presence of both HII and LINER or both HII and Sy spectral features [18].

Em. Spectra with relatively low quality where one or several emission lines are observed without a possibility of accurate classification. These spectra typically

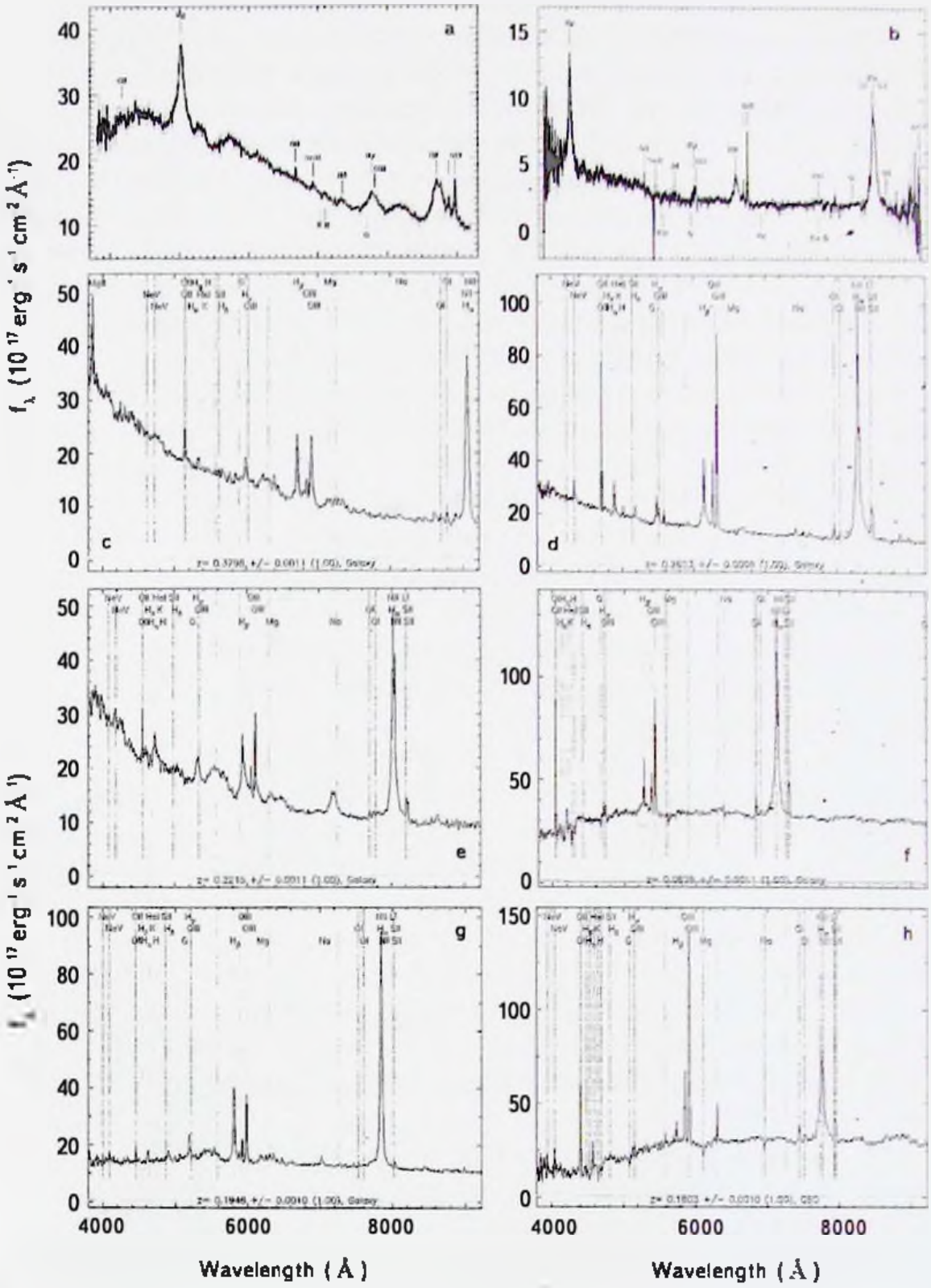

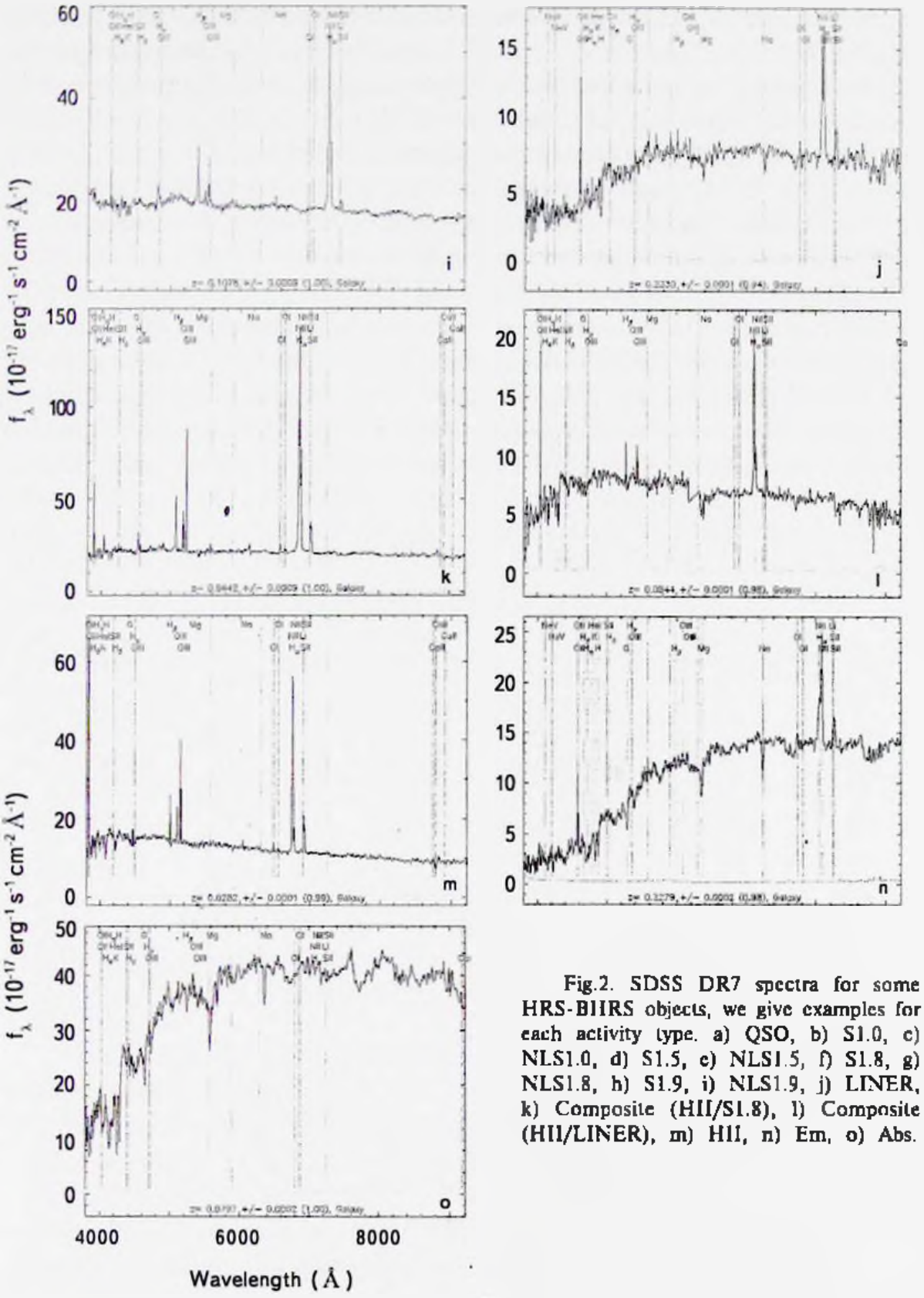

Fig.2. SDSS DR7 spectra for some HRS-BIIRS objects, we give examples for each activity type. a) QSO, b) S1.0, c) NLS1.0, d) S1.5, e) NLS1.5, f) S1.8, g) NLS1.8, h) S1.9, i) NLS1.9, j) LINER, k) Composite (HII/S1.8), l) Composite (HII/LINER), m) HII, n) Em, o) Abs.

have strong stellar component, and emission lines are hardly noticed above the continuum and absorption-line spectrum.

4. ***Results of study of spectra and classification.*** We started studying spectra with identifications of spectral lines. We have used only lines having intensities 3σ over the noise level. HIβ also appears in absorption on most of these spectra. We studied the influence of HIβ absorption component on the emission one, which is important for using of the numerical data given in SDSS tables. After identifications of the emission lines we decided which of them should be used to build diagnostic diagrams. Altogether 553 spectral lines were selected (7 lines from each of 79 emission line objects), but only 502 of them were used (77 HIβ, 77 [OIII] 5007 Å, 70 [OI] 6300 Å, 71 HIα, 71 [NII]6583 Å, 68 [SII] 6717 Å, 68 [SII] 6731 Å). As a result, we could build diagnostic diagrams using [OIII]/HIβ and [NII]/HIα ratios for 68 objects, [OIII]/HIβ and [OI]/HIα ratios for 64 objects, [OIII]/HIβ and [SII]/HIα ratios for 66 objects. In addition, we have identified following spectral lines important for AGN, which are not given in SDSS tables: [NeIII] 3869 Å, [NeIII] 3968 Å, [SII] 4069/76 Å, HeI 4471 Å, HeII 4686 Å, NI 5198/5200 Å, [NII] 5755 Å, HeI 5876 Å, [FeVII] 6087 Å, HeI 6678 Å, HeI 7065 Å, [ArIII] 7136 Å, [ArIV] 7237 Å, [OII] 7319 Å, [OII]

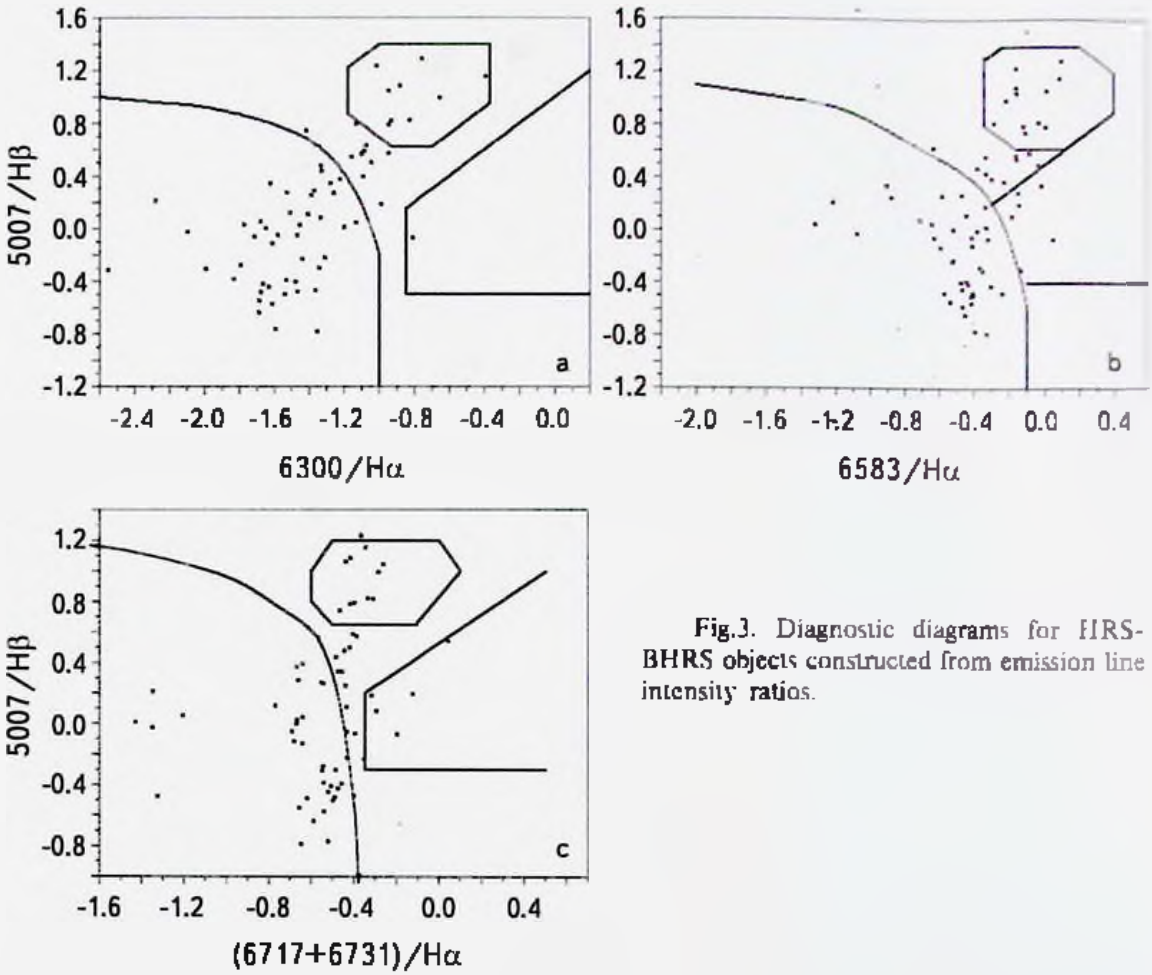

Fig.3. Diagnostic diagrams for HRS-BHRS objects constructed from emission line intensity ratios.

7329 Å . More often the forbidden lines appear in AGN spectra and permitted lines are stronger for HII galaxies.

We give in Fig.3 the diagnostic diagrams: in the diagnostic diagram a) we used [OI]/Hα and [OIII]/Hβ line intensities ratios, for the diagnostic diagram b) [NII]/Hα and [OIII]/Hβ line intensities ratios. and for the diagnostic diagram c) we used [SII]/Hα and [OIII]/Hβ line intensities ratios [11].

On diagnostic diagrams the narrow-line AGN are separated into 3 main groups (HII, Sy, LINER). In addition, there are objects in intermediate areas, which have been classified as Composites [11] having both AGN and HII features.

As a result of classification both from the diagnostic diagrams and by eye examination of all spectra, 4 (2.3%) QSOs, 42 (24.3%) Seyfert galaxies, 1 (0.6%) LINER, 6 (3.5%) Composite spectrum objects, 26 (15.0%) HIIs, 17 (9.8%) other Emission-line galaxies, and 66 (38.2%) Absorption-line galaxies (possible hidden AGN) have been revealed among these 173 objects (Table 1).

Table 1

DISTRIBUTION OF THE STUDIED 173 OBJECTS BY ACTIVITY TYPES

Activity type	Number of objects	Activity type	Number of objects
QSO	4	LINER	1
S1.0	1	LINER/Sy	1
NLS1.0	1	HII/Sy	1
S1.5	3	HII/LINER	4
NLS1.5	3	HII	26
S1.8	12	Em	17
NLS1.8	10	Abs	66
S1.9	10	Star	3
NLS1.9	2	UnCl	8

Note, that 41 of our objects have classification in NED. We reclassified these objects as well.

Table 2 lists the parameters of the main emission lines of the HRC-BHRC galaxies studied here. We have left only lines having 3σ over the noise level. The successive columns list the names of the objects, line intensities, the FWHM, EW, respectively for the spectral lines [OII] 3727 Å , Hβ , [OIII] 4959 Å , [OIII] 5007 Å , [OI] 6300 Å , [NII] 6548 Å , Hα , [NII]6583 Å , [SII] 6716 Å and [SII] 6731 Å . Next columns list [OIII]/Hβ , [OI]/Hα , [NII]/Hα , [SII]/Hα line intensities ratios, activity types based on these ratios or direct classification from spectra and activity types based on NED. These all parameters are given for 79 HRC-BHRC objects having measured line parameters in SDSS DR7-DR9.

4253 HRC-BHRC objects have been cross-correlated with SDSS DR7- DR9

*Table 2**

LISTS OF PARAMETERS OF THE MAIN EMISSION LINES OF THE HRC-BHRC GALAXIES

N			1	2	3	4	5	6
	Ions	Wave-length	J013205.2+024001	J090532.5+233505	J091707.4+210058	J093846.3+202459	J095123.4+220723	J095329.3+221020
Height	[OII]	3727	11.040	6.411	24.424	-8.014	13.862	13.813
	Hβ	4862	146.100	4.810	28.396	4.774	37.162	12.844
	[OIII]	4959	45.520	1.084	25.668	4.513	11.212	8.331
	[OIII]	5007	137.900	2.885	85.112	11.834	37.171	24.826
	[OI]	6300	4.369	0.904	4.301	2.060	3.488	2.118
	[NII]	6548	2.418	1.838	20.193	11.892	45.894	18.406
	Hα	6563	545.400	18.445	92.859	25.557	155.402	49.820
	[NII]	6583	45.970	5.617	38.929	12.842	64.932	35.352
	[SII]	6716	12.490	4.393	18.373	3.579	19.353	5.713
	[SII]	6731	11.900	2.445	14.963	2.254	13.937	5.171
EW	[OII]	3727	2.359	12.241	2.853	0.674	3.190	3.843
	Hβ	4862	34.401	6.788	3.124	7.375	13.104	5.927
	[OIII]	4959	11.038	2.701	2.779	1.362	4.713	3.117
	[OIII]	5007	33.932	5.992	9.756	5.063	16.202	11.094
	[OI]	6300	1.241	3.025	0.554	0.311	1.089	1.164
	[NII]	6548	0.706	3.333	10.795	21.098	27.747	28.768
	Hα	6563	159.567	40.184	17.013	33.782	78.083	48.638
	[NII]	6583	13.481	13.570	17.759	21.416	29.151	54.338
	[SII]	6716	3.717	6.647	5.964	5.964	6.647	5.964
	[SII]	6731	3.548	7.103	2.078	1.368	4.137	4.003
FWHM	[OII]	3727	369.471	311.174	244.190	487.539	379.755	460.809
	Hβ	4862	1527.572	227.714	225.359	1332.285	652.889	487.418
	[OIII]	4959	369.471	362.389	202.587	259.442	731.905	337.084
	[OIII]	5007	369.471	303.171	218.012	361.975	744.752	404.832
	[OI]	6300	369.471	247.573	204.809	69.413	417.306	278.500
	[NII]	6548	369.471	190.882	862.637	862.918	801.617	862.703
	Hα	6563	1527.572	242.159	265.268	642.100	659.089	449.955
	[NII]	6583	369.471	260.473	648.454	789.681	592.522	773.372
	[SII]	6716	369.471	261.856	207.479	243.622	389.354	372.835
	[SII]	6731	369.471	297.245	206.669	280.180	377.579	342.031
Ratio		[OIII]/Hβ	-0.025	-0.222	0.477	0.394	0.000	0.286
		[OI]/Hα	-2.096	-1.310	-1.334	-1.094	-1.649	-1.371
		[NII]/Hα	-1.074	-0.516	-0.378	-0.299	-0.379	-0.149
		[SII]/Hα	-1.350	-0.431	-0.445	-0.642	-0.669	-0.661
Class			NLS 1.8	HII	Sy 1.8	NLS 1.8	HII	NLS 1.5
NED			n/a	n/a	Sy 1	QSO	Sy 1.2	QSO

* Complete Table 2 is given only in electronic form in Vizier database of astronomical catalogues.

with the search radius of 10 arcsec. 156 spectra have been obtained from SDSS DR7, 8 additional spectra from DR8 and 9 additional spectra from DR9. The lowest SDSS redshift for these objects is 0.004 and the highest is 2.865. The average redshift is 0.224.The distribution of these redshifts is given in Fig.4. As we see in Fig.4 the redshifts of the most of objects are between 0.02 and 0.20. The average values of SDSS u, g, r, i, z magnitudes for these objects are 18.94, 17.53, 16.75, 16.36 and 16.10, respectively.

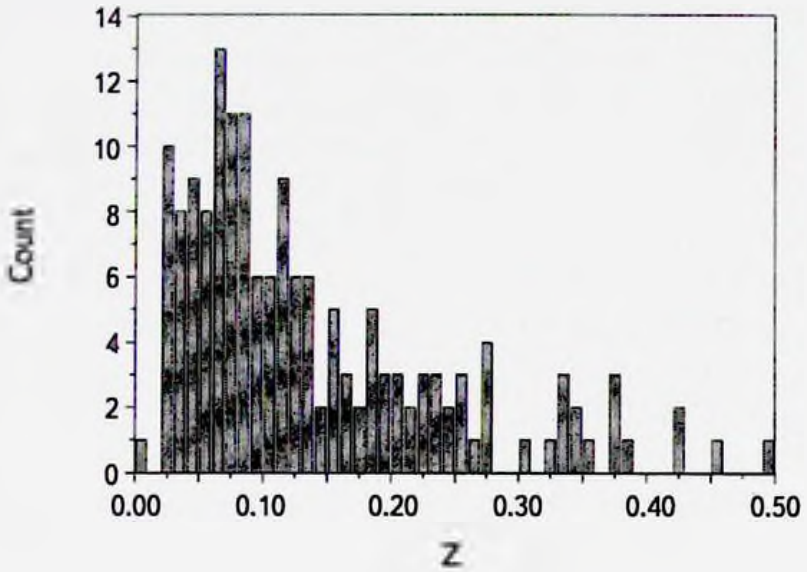

Fig.4. The distribution of redshifts for 173 X-ray sources.

5. *Multiwavelength data*. These 173 objects have been cross-correlated with GALEX [19] UV catalog with a search radius of 30 arcsec: 91 objects have been cross-matched; 42 of them on a distance of 1 arcsec and 49 objects on 2.5 arcsec distance. The average values of fluxes at GALEX FUV and NUV bands are 20.14 mag and 19.89 mag respectively.

173 objects having spectra on SDSS have been cross-correlated with 2MASS [20] NIR catalog with a search radius of 30 arcsec. 138 objects have been found between 0.02 arcsec and 1.74 arcsec with average radius of 0.38 arcsec. The average values of 2MASS J, H, K magnitudes for these objects are 15.31, 14.59 and 14.07, respectively.

The 173 objects have been cross-correlated with All WISE [21] NIR/MIR catalog with a search radius of 25 arcsec: 171 objects have been cross-matched; 161 of them on a distance of 1 arcsec and 10 objects on 1.9 arcsec distance. The average values of magnitudes at WISE W1, W2, W3, and W4 bands are 13.61, 13.28, 11.12 and 8.45, respectively.

These 173 HRC-BHRC objects have been cross-correlated with IRAS PSC [22] and FSC [23] with a search radius of 100 arcsec and 7 objects have been found.

*Table 3***

DIFFERENT PARAMETERS OF OUR SAMPLE BASED ON RESULTS OF CROSS-MATCHING WITH MULTIWAVELENGTH CATALOGS

N	1	2	3	4	5	6	7
IRXS	J003128.0 +022525	J142424.8 +251427	J095329.3 +221020	J132409.9 +135855	J084800.4 +314648	J170045.9 +291925	J151104.5 +112137
CR(cr/s)	0.0463	0.082	0.0423	0.055	0.0407	0.098	0.14
HR 1	0.44	0.16	0.52	0.58	0.3	0.72	-0.23
HR 2	-0.05	-0.1	-0.27	0.17	0.08	0.08	0.3
F_x(mW/m^2)	4.93E-13	7.51E-13	4.68E-13	6.26E-13	4.03E-13	1.19E-12	9.93E-13
RAJ(deg)	7.86515	216.1011	148.3609	201.0418	131.9960	255.1949	227.761
DEJ(deg)	2.43616	25.24101	22.17054	13.9765	31.78566	29.32405	11.36283
u (mag)	18.635	19.305	18.387	14.756	16.494	17.721	17.989
g (mag)	17.120	18.146	18.474	12.792	14.465	16.355	17.620
r (mag)	16.335	17.345	18.159	11.946	13.536	15.597	17.410
i (mag)	15.849	16.878	17.829	11.575	13.064	15.129	16.876
z (mag)	15.508	16.776	17.749	11.273	12.737	14.807	16.998
z (redshift)	0.078536	0.233124	0.221736	0.022968	0.067306	0.06827	0.112806
GALEX-SDSS(as)	1.005	0.42	0.752	1.301	0.405		2.5
FUV(mag)	21.221	19.657	18.262	19.631	21.363		19.416
NUV(mag)	20.058	19.348	18.036	18.035	19.984		18.817
2MASS-SDSS(as)	0.366	1.049	0.111	1.344	0.346	0.239	0.233
J(mag)	14.922	15.629	16.485	12.125	13.8	14.407	15.97
H(mag)	14.061	14.883	15.765	11.408	13.376	13.591	15.207
K(mag)	13.54	15.293	14.705	11.122	12.794	13.115	14.175
IRAS-SDSS(as)	36.3		13.1			16.8	
F_{12}(Jy)	0.25		0.07442			0.069	
F_{25}(Jy)	0.4573		0.2131			0.08875	
F_{60}(Jy)	0.4215		0.1602			0.2133	
F_{100}(Jy)	1		0.5504			1.099	
WISE-SDSS(as)	0.43	0.868	0.159	1.712	0.306	0.255	0.13
W1(mag)	12.83	13.90	13.66	10.15	11.25	12.26	12.98
W2(mag)	12.51	13.49	12.73	10.20	11.28	11.96	12.00
W3(mag)	8.51	10.62	9.26	9.71	10.63	8.79	8.78
W4(mag)	5.88	8.73	6.48	8.08	8.46	6.42	6.21
NVSS-SDSS(as)	2.04	1.52		4.99	8.53	6.99	
S_{1400}(mJy)	4	6.9		7.2	45	2.5	
FIRST-SDSS(as)	0.617	0.244		1.444	0.355	0.161	0.248
F_{peak}(mJy)	2.99	6.12		4.65	25.56	1.81	2.72
F_{int}(mJy)	2.63	7.36		4.88	25.98	1.8	2.49
V (km/sec)	22638.25	61960.95	59291.24	6811.29	1567.88	19783.40	31943.87
D(Mpc)	325.845	932.466	889.373	96.493	22.1001	283.916	464.344
L_x(W)	7.28E+35	1.19E+37	6.61E+36	7.30E−34	2.38E+33	1.31E−36	3.17E−36
L_r(W)	6.64E+36	2.80E+37	1.18E+37	9.40E+36	9.94E−34	9.75E−36	5.33E−36
M_r(mag)	-21.27	-22.73	-21.81	-21.76	-16.86	-21.71	-21.06
Activity type	HII	LINER	NLS1.5	ABS	Em	Sy1.9	NLS1.8

** Complete Table 3 is given only in electronic form in Vizier database of astronomical catalogues.

The average distance of cross-matching was 20.15 arcsec. The average values of fluxes of these objects at 12, 25, 60 and 100 μ wavelengths are 0.21 Jy, 0.24 Jy, 0.29 Jy and 1.86 Jy, respectively. Here we did not use fluxes given with upper limits, i.e. without exact measurements.

These objects have been cross-correlated with NVSS [24] radio catalog as well. 38 objects out 41 associated have been cross-matched in 30 arcsec radius. The average flux at 21 cm is 33.48 mJy.

173 HRC-BHRC objects have been cross-correlated with the FIRST [25] radio catalog. 42 objects have been found in 1 arcsec radius, 10 of them are in 3 arcsec radius. The average FIRST integral flux is 23.85 mJy (FIRST also gives the peak flux, which is a signature of the shape of the radio source, but this does not match with NVSS fluxes and the total luminosity).

Table 3 lists different parameters of our sample based on results of cross-matching with multiwavelength catalogs. The successive columns list the ROSAT data (ROSAT name of the object, count rate, hardness ratio 1, hardness ratio 2, X-ray flux), SDSS data (RA and DE J2000, u, g, r, i, z mag, redshift), GALEX data (cross-matching distance, FUV, NUV mag), 2MASS data (cross-matching distance, J, H, K mag), IRAS (cross-matching distance, f12, f25, f60, f100 Jy), WISE data (cross-matching distance, S65, S90, S140, S160 Jy), NVSS data (cross-matching distance, S1.4 in mJy), FIRST data (cross-matching distance, F_{peak}, F_{int} in mJy), radial velocity, distance (H = 72), luminosities, M_r mag and activity type for each of our sample objects.

We give in Table 4 the average parameters for our 162 objects, having definite activity types. The successive columns list the activity types, numbers, average redshifts, average absolute M_r magnitudes, average u-g and g-r colors, and X-ray/opt flux ratios for AGN (QSO+Sy+LINER), Composites, HIIs, Em and Abs galaxies.

All AGN (Sy+LINER) and Composites together in average have redshift 0.391, which is 1.8 times higher than that for HIIs. The average absolute magnitude of all AGN and Composites together is $M_r = -22.18$, which is smaller

Table 4

MEAN PHYSICAL PARAMETERS OF HRC-BHRC OBJECTS OF DIFFERENT ACTIVITY TYPES

Activity type	Number of objects	<Redshift>	HR1	M_r	u-g	g-r	$\lg(F_x/F_{opt})$
QSO+Sy+LINER	47	0.347	-0.09	-22.11	0.74	0.54	-0.50
Composite	6	0.061	0.16	-21.32	1.19	0.53	-0.77
HII	26	0.078	-0.13	-22.02	1.14	0.56	-0.92
Em	17	0.126	0.34	-22.41	1.74	0.95	-0.83
Abs	66	0.125	0.49	-22.55	2.05	1.09	-0.98

than that for HIIs by 0.39 $M_\odot$. The average u-g color for all AGN and Composites together is 0.95 and that for HIIs is $1^m.15$. The average g-r color for all AGN and Composites together is $0^m.52$ and that for HIIs is $0^m.57$.

The radial velocities of our sample of objects are between 6800-245851 km/s, the distances are between 96-5410 Mpc, the M_r absolute magnitudes are between -16.68 to -30.36.

In Fig.5, we give the distribution of objects by log(CR)+0.4r vs r. It is especially interesting to consider these ratios for absorption line galaxies to understand if they have hidden AGN or have X-ray flux due to the integral galactic radiation. The AGN distribution is on a discrete area between the line A (log(CR) + 0.4r = 4.9) and the line B (log(CR) + 0.4r = 6.4) [26].

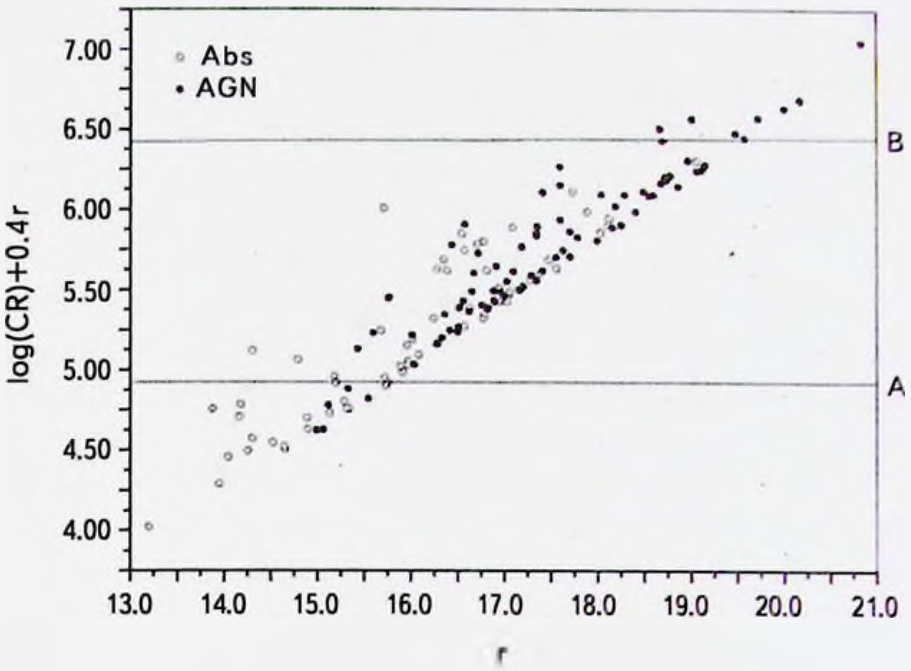

Fig.5. The distribution of combined X-ray count rate (in logarithmic scale) and SDSS r magnitude vs. SDSS r magnitude.

This way we have found 50 (between line A and B) objects that may be suspected to have hidden AGN.

6. *Summary and Conclusion*. We have created a large homogeneous sample of X-ray selected AGN and carried out spectroscopic investigation for those objects having SDSS spectra. 173 objects appear in this list and we have classified them by activity types using three diagnostic diagrams and eye examination of the spectra (to be complete in classification of broad line AGN). Many Seyferts, LINERs, Composites and Starburst have been revealed. We have applied all possible parameters for fine classification to distinguish between narrow and

classical broad line Seyferts, and to identify all details related to Seyfert subtypes depending on the strength of their broad components. We have introduced subtypes of NLS1, namely NLS1.0, NLS1.2, NLS1,5 and NLS1.8 giving more importance to these details. Further accumulation of statistics may provide possibilities to understand the physical differences.

We have calculated all possible physical parameters of the studied objects: radial velocities, distances, absolute magnitudes, luminosities, etc.

One of the most intriguing class of objects among the X-ray sources are absorption line galaxies. The brightest ones may just appear in this sample due to their integral high luminosity, however we find that many such objects have low luminosity and still appear to be strong X-ray sources. We consider these objects as possible hidden AGN. The optical spectra do not show any signatures of emission.

The spectroscopic classification and study led to the revelation of many new AGN and Starburst, and our sample contents became more reliable, also taking into account the previously known objects collected from NED. Out of the 4253 HRC-BHRC objects, 3369 sources were confirmed as AGN by previous spectroscopic observations, and we have added 173 new ones (though some were reclassified).

We have constructed X-ray/opt flux ratios diagram to distinguish strong X-ray sources and hidden AGN. 50 objects prove to be hidden AGN due to their strong X-ray, relatively weak optical flux and absence of any emission line features in optical spectra. We have also carried out multiwavelength cross-correlations to follow the SEDs of these objects and understand their behavior also in other wavelength ranges.

Acknowledgements. The authors are very grateful for the helpful comments and suggestions of the anonymous referee. The only disagreement with the referee remained the issue concerning the objects referred here as hidden AGN's and considered as galaxy clusters by the referee. We continue to believe on their galactic nature, since the objects are observed as separate galaxies from the SLOAN Survey. Further studies of the issue will solve this question as well.

[1] NAS RA V.A.Ambartsumian Byurakan Astrophysical Observatory (BAO), Armenia, e-mail: gurgen_paronyan@yahoo.com
[2] Leibniz-Institutfur Astrophysik Potsdam (AIP), Germany

ТИПЫ АКТИВНОСТИ ГАЛАКТИК, ОТОБРАННЫХ ИЗ ВЫБОРКИ HRC-BHRC

Г.М.ПАРОНЯН, А.М.МИКАЕЛЯН, Г.С.АРУТЮНЯН, А.В.АБРАМЯН, Г.А.МИКАЕЛЯН

В этой работе мы проводим детальную спектральную классификацию 173 кандидатов AGN из объединенной выборки HRC/BHRC, которая представляет собой комбинацию HRC (каталог Гамбург-ROSAT) и BHRC (каталог Бюракан-Гамбург-ROSAT). Эти объекты были выявлены как оптические отождествления для рентгеновских источников ROSAT, однако спектры для 173 из них приведены в SDSS без определенной спектральной классификации. Мы изучили эти 173 объекта с использованием спектров SDSS и выявили для них подробные типы активности. Для более уверенной классификации использовались три диагностические диаграммы и прямое исследование спектров. Мы также отождествили эти источники в других диапазонах длин волн и вычислили некоторые их параметры.

Ключевые слова: *AGN:рентгеновское излучение:спектральная классификация. HRC/BHRC: рентгеновские AGN*

REFERENCES

1. *W.Voges, B.Aschenbach, Th.Boller al.*, Astron. Astrophys., **349**, 389, 1999.
2. *W.Voges, B.Aschenbach, Th.Boller al.*, IAU Circ. 7432R, 2000.
3. *A.Schwope, G.Hasinger, I.Lehmann et al.*, AN, **321**, 1, 2000.
4. *H.-J.Hagen, D.Groote, D.Engels et al.*, Astrophys. J. Suppl. Ser., 111, 195, 1995.
5. *F.-J.Zickgraf, D.Engels, H.-J.Hagen et al.*, Astron. Astrophys., **406**. 535, 2003.
6. *A.M.Mickaelian, L.R.Hovhannisyan, D.Engels et al.*, Astron. Astrophys., 449, 425, 2006.
7. *M.P.Veron-Cetty, P.Veron*, Astron. Astrophys., **518**, A10, 2010.
8. *E.Massaro, P.Giommi, C.Leto et al.*, Astron. Astrophys., **495**, 691, 2009.
9. *C.P.Ahn, R.Alexandroff, C.Allende Prieto et al.*, Astrophys. J. Suppl. Ser., **211**, 17, 2014.
10. *K.Abazajian et al.*, Astrophys. J. Suppl. Ser., **182**, 543, 2009.
11. *S.Veilleux, D.E.Osterbrock*, Astrophys. J. Suppl. Ser., **63**, 295, 1987.
12. *D.E.Osterbrock*, Proc. Texas Symposium on Relativistic Astrophysics, 9th Munich, West Germany, Dec 14-19, 1978, New York, New York Academy of Sciences, 1980, p.22.

13. *H.Winkler*, Mon. Not. Roy. Astron. Soc., **257**, 677, 1992.
14. *D.E.Osterbrock, R.W.Pogge*, Astrophys. J., **297**, 166, 1985.
15. *T.M.Heckman*, Astron. Astrophys., **87**, 152, 1980.
16. *L.C.Ho, A.V.Filippenko et al.*, Proceedings of IAU Colloquium No. 159, 1997.
17. *D.W.Weedman*, Vistas in Astronomy, **21**, 55, 1977.
18. *P.Veron, A.C.Goncalves, M.P.Veron-Cetty*, Astron. Astrophys., **319**, 52, 1997.
19. *L.Bianchi, J.Herald, B.Efremova et al.*, Astrophys. J. Suppl. Ser., **335**, 161, 2011.
20. *M.F.Skrutskie, R.M.Cutri, R.Stiening et al.*, Astron. J., **131**, 1163, 2006.
21. *R.M.Cutri et al.*, IPAC/Caltech, 2013.
22. *C.A.Beichman, G.Neugebauer, H.J.Habing et al.*, IRAS catalogs and atlases, 1988.
23. *M.Moshir et al.*, IRAS Faint Source Survey, JPL D-10015 8/92, (IPAC), 1992.
24. *J.J.Condon, W.D.Cotton, E.W.Greisen et al.*, Astron. J., **115**, 1693, 1998.
25. *R.H.Becker, D.J.Helfand, R.L.White et al.*, Astrophys. J., **475**, 479, 1997.
26. *L.Cao, J.-Y.Wei, J.-Y.Hu*, A&AS, **135**, 243, 1999.